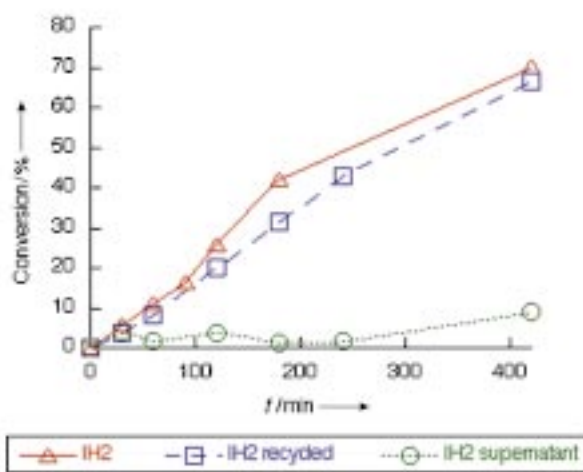
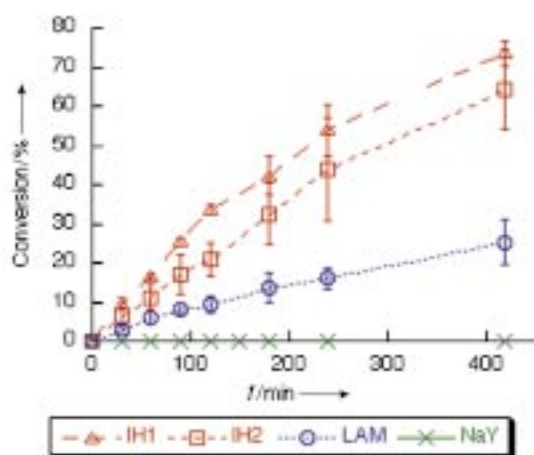
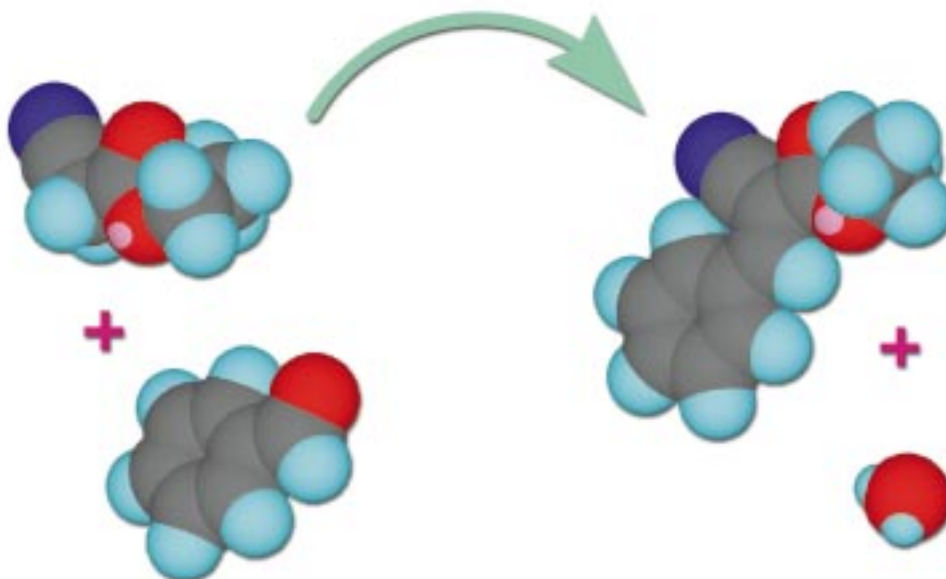
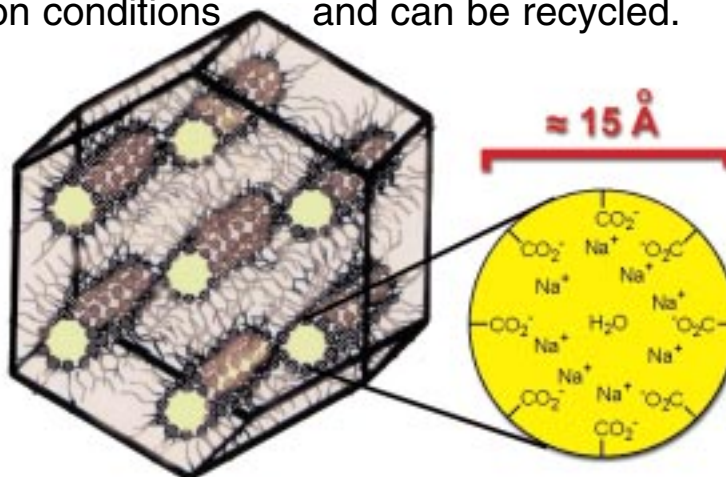


Organic zeolites ?

Nanostructures self-assembled from lyotropic liquid crystals can be stabilized by polymerization and used as base catalysts. The active sites in these assemblies are highly accessible, and the materials maintain order in reaction conditions and can be recycled.

More about this on the following pages



Heterogeneous Catalysis with Cross-Linked Lyotropic Liquid Crystal Assemblies: Organic Analogues to Zeolites and Mesoporous Sieves**

Seth A. Miller, Esther Kim, David H. Gray, and Douglas L. Gin*

The angstrom- and nanoscale structure of catalysts can dramatically alter their reactivity, selectivity, and efficiency. Zeolites, a class of crystalline aluminosilicates with uniform channels in the range of 3 to 15 Å, represent the pinnacle of nanostructured catalyst design (Figure 1 a).^[1] These materials

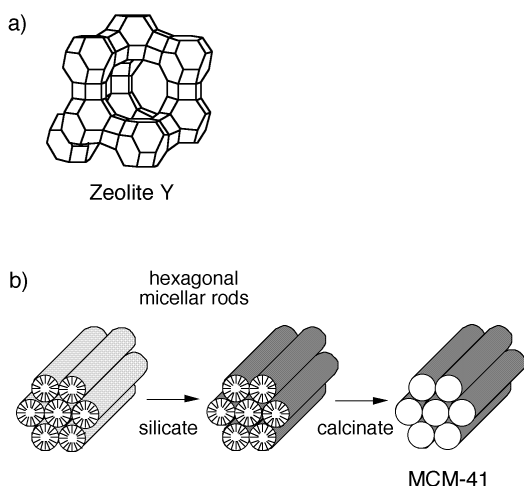


Figure 1. Nanoporous inorganic catalysts with regular structures: a) Zeolite Y, b) MCM-41.

exhibit high reactivity, recyclability, remarkable shape selectivity, and stability under extreme conditions. Consequently, they have been widely adopted as catalysts by industry for processes such as petroleum cracking and methane oxidation.^[2] However, zeolites are not amenable to processing, and their pore sizes and architectures are not easily adjustable for modulating reactivity. As a result, there has been considerable effort to find and develop materials that mimic the structure, reactivity, and selectivity of zeolites, but offer more control. For example, much attention has recently been given to mesoporous sieves, a family of templated silicate structures with tunable pore sizes from 20 to 100 Å (Figure 1 b).^[3] They have been explored with an eye towards novel reactivities but

their lack of stability in hydrolytic environments and low reactivity have so far prevented their adoption in industrial catalytic applications.^[4]

Organic analogues to zeolites and mesoporous sieves have been pursued with the goal of using the power of organic synthesis to tune the reactivity, processability, and architecture of the resulting systems. For example, noncovalent, crystalline organic supercages have been made that are highly porous and able to accommodate a variety of guests.^[5] These systems, however, are typically not stable to solvent or to removal of the guests. Cross-linked reverse microemulsions have successfully been used as heterogeneous organic catalysts for reactions such as phosphate hydrolysis.^[6] However, they too lack the selectivity and activity needed for many catalysis applications.

We present here a new class of catalytically active, nanoporous organic materials based on cross-linked lyotropic liquid crystals (LLCs). These solids have regular channel structures similar to those of mesoporous sieves but with much higher intrinsic reactivity. Size exclusion by the mesopores and enhanced basicity result from the nanoscale organization of the functional groups making up the channel walls. The activity of the materials is dependent on the channel structure. These materials function as efficient heterogeneous base catalysts for the Knoevenagel condensation.

Lyotropic liquid crystals are molecules composed of a polar head group and a hydrocarbon tail. Upon addition of water, these systems self-organize into phase-separated assemblies such as spheres, ordered cylinders, interconnected channels, and lamellae.^[7] We have used the LLC monomer **1**,^[8] which can pack into a lamellar or inverted hexagonal structure depending on the amount of water added.^[9] In the case of an inverted hexagonal structure, the carboxylate groups and their counterions pack densely together around extended aqueous channels approximately 10–15 Å in diameter to form a close-packed assembly of ions surrounded by a continuous organic medium (Figure 2).^[10] Monomer **1** contains a polymerizable styryl group, and upon addition of divinylbenzene (12 wt %), **1** can be photo-cross-linked into a “rigid” covalent polymer network that maintains the nanoscale order of the original LLC phase.^[8]

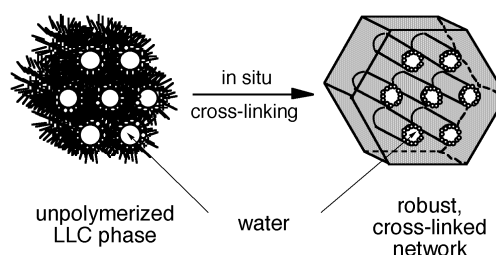
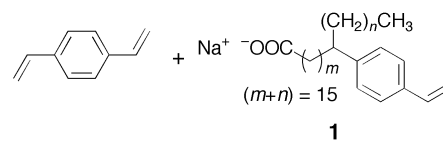
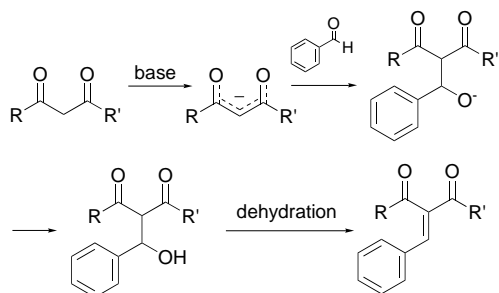


Figure 2. Synthesis of the cross-linked inverted hexagonal LLC phase using monomer **1** (a mixture of regioisomers).^[8]

[*] Prof. D. L. Gin, Dr. S. A. Miller, E. Kim, D. H. Gray
Department of Chemistry
University of California
Berkeley, California 94720 (USA)
Fax: (+1) 510-643-1846
E-mail: gin@cchem.berkeley.edu

[**] Financial support for this work was provided by the Office of Naval Research (N00014-97-1-0207), the Donors of the Petroleum Research Fund (33632-AC5,7), and the Exxon Education Fund. We would like to thank Dr. Jacek Klinowski of Cambridge University for supplying a sample of Na-MCM-41 and Zeolyst International for samples of NaY. We also thank Prof. Robert G. Bergman for helpful discussions at the initial stages of this project.

Cross-linked **1** was initially studied as a potential heterogeneous base catalyst, since the aqueous channels are lined with weakly basic carboxylate groups ($pK_a \approx 4.7$ in H_2O). Increased basicity may arise from the close packing of these charged groups inside the nanometer-scale pores. The Knoevenagel condensation of ethyl cyanoacetate with benzaldehyde (Scheme 1) was chosen as an initial test reaction of base



Scheme 1. Hann–Lapworth mechanism of the Knoevenagel condensation.^[23]

catalysis for two reasons: 1) This condensation is well-known to be catalyzed by weak bases,^[11] and the kinetics of the reaction can easily be modulated by changing the starting materials, temperature, or solvent;^[12] 2) This reaction has been previously examined using sodium-exchanged zeolite Y (NaY),^[13] mesoporous sieve (Na-MCM-41),^[14] and amine-modified MCM-41^[15] as catalysts. Thus, direct comparisons can be made between cross-linked **1** and existing inorganic, nanostructured catalysts.

The stability of cross-linked **1** was assessed before any kinetic experiments were run. Three batches of cross-linked **1** were prepared containing 8 (IH1), 15 (IH2), and 30 wt % water (LAM). Powder X-ray diffraction of these cross-linked phases showed IH1 and IH2 to be inverted hexagonal and LAM to be lamellar, as indicated by characteristic diffraction spacings of $(1, 1/\sqrt{3}, 1/2, \dots)$ and $(1, 1/2, 1/3, \dots)$, respectively.^[8] Each cross-linked phase was extracted with dry THF at reflux for four hours and retrieved by filtration under a nitrogen atmosphere. The inverted hexagonal matrices (IH1 and IH2) showed a slight decrease in overall order, as indicated by broadening of the X-ray diffraction peaks. However, their diffraction patterns and d-spacings are essentially similar (Figure 3). In contrast, the lamellar phase (LAM) showed greater disorder after cleaning, probably due to the tremendous volume loss as unbound water was removed from the matrix by THF extraction.

Phases IH1, IH2, and LAM were tested as base catalysts for the condensation of ethyl cyanoacetate with benzaldehyde (Scheme 1). The reaction was initially examined in water at reflux ($100^\circ C$), neat at room temperature, and in THF at reflux ($66^\circ C$) using 5 mol % catalyst loading. The reaction in water at reflux was highly efficient, with nearly quantitative conversion into products in only 15 min. In comparison, the use of Na-MCM-41 (5 mol %) under identical conditions in refluxing water yielded the product in 90 % yield after three hours.^[14] This was, however, too fast for a detailed kinetic analysis of our system. Running the reaction in THF allowed

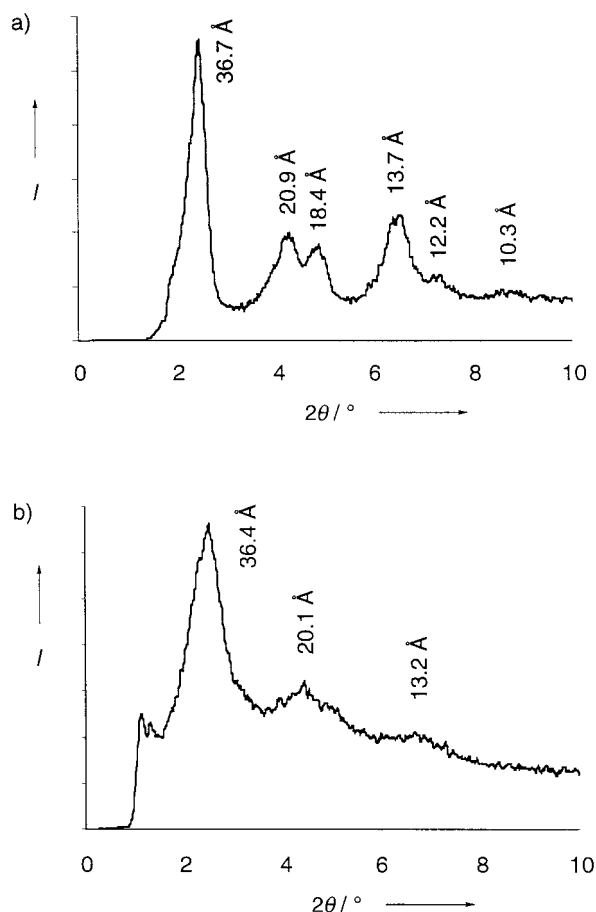


Figure 3. Powder X-ray diffraction profiles of IH1 a) before and b) after boiling in THF. After boiling in THF, the closely spaced peaks have grown together, but the spacing patterns are still indicative of an inverted hexagonal phase.

convenient monitoring of the reaction progress by gas chromatography (GC), and allowed for differentiation of the reactivities of each matrix and the NaY and Na-MCM-41 controls. In addition, 2 % cross-linked sodium polyacrylate was used as a secondary control in order to account for 1) any intrinsic basicity differences between carboxylates and anionic aluminosilicates, and 2) to compare an amorphous carboxylate system with one ordered into nanopores. The results reported below are for the reactions in THF, except where otherwise indicated.

The results of the runs in THF are shown in Figure 4. Phases IH1 and IH2 are first-order (a linear plot of $\ln c$ vs. t) with statistically equivalent rate constants ($k = 0.003$), but both show significantly more activity than LAM ($k = 0.001$). Na-MCM-41, NaY, and cross-linked sodium polyacrylate containing the same number of basic sites (as determined by elemental analysis for Na) show no activity under these conditions. In contrast, a reaction using sodium oleate as a homogeneous catalyst is second-order (a linear plot of $1/c$ vs. t) with respect to reactants, consistent with a bimolecular rate-limiting step in solution. The first-order rate constant for the LLC matrices indicates that deprotonation may be rate-limiting, and the reaction likely proceeds in a mass transport limited regime. No changes in reaction rate were seen by

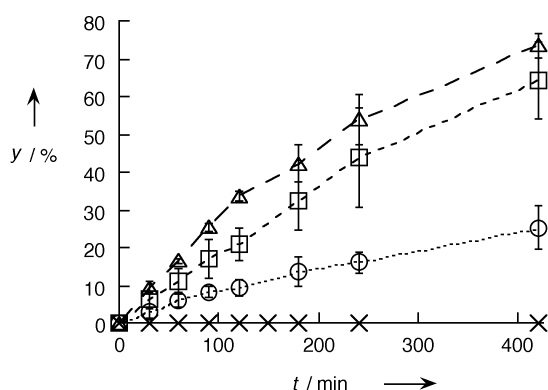


Figure 4. Results of the Knoevenagel condensation in refluxing THF; each point is the average of three runs. IH1 (Δ), IH2 (\square), LAM (\circ), NaY (\times); y = conversion. Na-MCM-41 and cross-linked sodium polyacrylate behave exactly as NaY.

varying the stirring rate, and the effect of particle size on reactivity could not be accurately assessed because the cross-linked particles were broken up over the course of the reaction. It is impossible to say whether the reactivities of NaY or Na-MCM-41 are so much lower due to limited transport or lower intrinsic basicities, although they are known to catalyze this reaction under more extreme conditions.^[13, 14]

Recycling experiments were performed to show that the catalytic activity of the cross-linked LLC matrices does not arise from soluble fractions leached out by the THF. After an initial reaction run, the supernatant was removed, filtered into a fresh flask, and charged with new reactants. The remaining solid was then washed and charged with fresh starting materials and THF. The supernatant repeatedly showed a very small but real activity as a base catalyst for the Knoevenagel reaction in THF. This activity was always considerably lower than that of the recycled solid, whose activity was not significantly degraded from that of the original run (Figure 5).

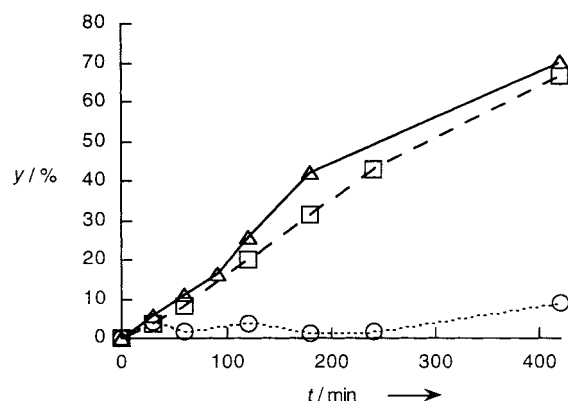


Figure 5. Recycling experiment for IH2. Original run of IH2 (Δ), recycled IH2 (\square), and the supernatant from the original run (\circ); y = conversion.

Phase IH2 was also tested as a catalyst for the condensation of ethyl cyanoacetate and benzaldehyde in the absence of solvent at room temperature; the catalyst loading level was 5 mol%. Reaction mixtures were stirred rapidly for two hours, then quenched by extracting the organic components

into ether, and analyzed by GC. Under these conditions, 70% of the starting material is converted into product by IH2. In contrast, Corma et al. showed that 20 wt% NaY in neat benzaldehyde and ethyl cyanoacetate only afforded 19% conversion after two hours at 140 °C.^[13] Since sodium oleate does not dissolve in neat benzaldehyde and ethyl cyanoacetate at room temperature, it was used as a nonporous heterogeneous control; it gives only 30% conversion after two hours. No product is seen using NaY or cross-linked sodium polyacrylate as heterogeneous catalysts in this neat system.

We rationalize these results in terms of two possible issues:

- 1) Basicity: Differences in the intrinsic basicity of the active sites (COO^- vs. aluminosilicate anions) may determine the ability of a system to catalyze the Knoevenagel condensation under certain conditions.
- 2) Accessibility: The LLC system under study is heavily cross-linked, and this may exclude species from the active sites. We anticipated the nanometer-scale order should keep the carboxylate groups largely accessible. However, size exclusion by the approximately 10–15 Å large pores may limit the ability of reagents to migrate into the channels, or the ability of products to leave the LLC matrix.

The basicity and accessibility of cross-linked **1** were determined by acid titration. Titration with strong acids yields the total amount of solvent-accessible basic groups, whereas titration with weaker acids shows the base strength of these sites. Previous studies of regular micelles containing carboxylate groups^[16] have generally shown increases in basicity from one to three $\text{p}K_a$ units, resulting from the decrease of the dielectric constant and an increase in surface potential as the ionic carboxylate groups pack together. Analogous work on close-packed, surface-exposed carboxylates have shown similar effects.^[17] These effects are not seen for unstructured polymers.^[18] Both volumetric and spectrophotometric methods were used in this work, and they yielded consistent results.

For the volumetric titration experiments, the three samples of cross-linked **1** (IH1, IH2, and LAM) were stirred in water containing two equivalents of acids of varying $\text{p}K_a$ values. After two days, an aliquot of the resulting supernatant liquid was titrated with sodium hydroxide, and the amount of acid absorbed by the matrices was determined. For weaker acids in water, **1** was stirred with one equivalent of phenol, 3-nitrophenol, or 4-nitrophenol in the absence of air, and the emergence of the deprotonated species was monitored by UV/Vis spectroscopy. The results of these experiments are summarized in Figure 6. The acids used for these volumetric titration experiments ranged in strength, from HCl to phenol ($\text{p}K_a$ range –7 to 10), and in ionicity (e.g. acetic acid, $\text{p}K_a = 4.7$, vs. pyridinium, $\text{p}K_a = 5.2$).

As can be seen in Figure 6, amorphous, cross-linked sodium polyacrylate behaves analogously to a free carboxylate group in solution. In addition, neither cross-linked sodium polyacrylate nor NaY deprotonate acids with $\text{p}K_a$ values greater than 6.8. However, nanostructured LLC networks IH1, IH2, and LAM deprotonated all the acids in this series. These experiments yielded two important results: 1) Approximately 80–90% of the carboxylate sites in the nanostructured LLC

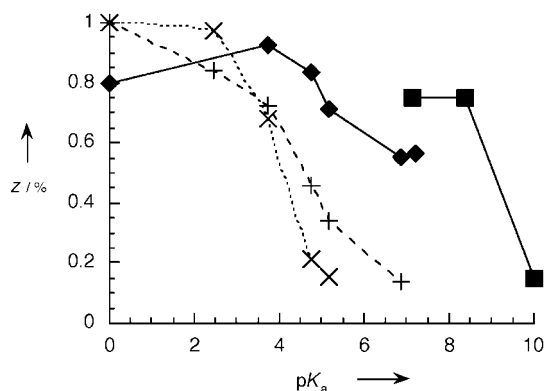


Figure 6. Titration of cross-linked LLC networks and controls in water. IH1 (♦), NaY (+), and cross-linked polyacrylic acid (X) were titrated volumetrically with acids of varying strength. IH1 was also titrated spectrophotometrically (■); z = amount of potential sites protonated.

networks (as determined from elemental analysis for Na) are accessible in water. 2) These sites are significantly more basic than those of amorphous carboxylate-containing polymers and NaY. The observed deprotonation of 4-nitrophenol ($pK_a=7$), 3-nitrophenol ($pK_a=8$), and phenol ($pK_a=10$) represents about five orders of magnitude greater apparent basicity than that of soluble carboxylate ions in water. This value is three orders of magnitude greater than that usually seen for micellar systems.^[16c] Such increased basicity likely arises from decreased stability of anions in the lower dielectric environment of the inverse hexagonal structures^[19] as well as an electrostatic effect from packing the carboxylates densely together.^[16a]

To account for the much lower catalytic activity exhibited by LAM compared to IH1 or IH2, experiments were performed to determine whether LAM differs owing to intrinsically lower basicity or lower accessibility as a result of its different nanostructure. For these experiments, each LLC matrix was boiled in THF for two hours with one equivalent of 4-nitrophenol ($pK_a=10.8$ in DMSO),^[20] and the amount of nitrophenoxide generated was assessed spectrophotometrically. Under these conditions, IH1 deprotonated 70% of the nitrophenol, compared with 30% deprotonated by LAM. Most strikingly, under the same conditions the LAM matrix only deprotonated 37% of the 2,4-dinitrophenol ($pK_a=5.1$ in DMSO).^[20] 2,4-Dinitrophenol is sufficiently acidic that it should easily protonate any accessible alkyl carboxylate group ($pK_a=11$ in DMSO). In THF, LAM appears to have equivalent basicity to IH1 and IH2 but fewer accessible carboxylate sites. The lower accessibility of the carboxylate groups in LAM fits well with the kinetic data, where the disappearance of about half of the active units correspondingly drops the catalytic rate by about a factor of two. This result also supports our model that nanostructural order in these materials is essential for obtaining high activity. The addition of water appears to swell the LAM matrix and can restore accessibility back to the level of IH1 and IH2.

Finally, simple size-exclusion experiments were performed on the cross-linked inverted hexagonal phase in order to get an indication of practical channel size selectivity independent of substrate reactivity. Extracted IH1 was stirred in water with

an excess of polycationic guest molecules of varying sizes, and the uptake by the anionic pore framework was monitored by UV/Vis or ^1H NMR spectroscopy (to determine the amount of remaining guests in the supernatant). Two polycations were chosen to encourage cation exchange by chelation. Alcian Blue (pyridine variant) is a fairly rigid tetracationic porphyrin-based dye with a diameter of approximately 15–20 Å, depending on its conformation. When one equivalent (based on cation content) of this compound is stirred with IH1, 7% of the dye is absorbed by the matrix after two hours and only 14% after two days. In contrast, over 70% of gallamine triiodide (1,2,3-tris[2-(triethylammonio)-ethoxy]-benzene triiodide), a smaller trication (<10 Å), was absorbed by the matrix after only one day. These two simple experiments confirm our rough estimate of the nanochannel size of 10–15 Å, and demonstrate that size exclusion may be one method to modulate catalytic activity. Given the small molecular size of our starting materials and products, it is unlikely that any sort of size exclusion is affecting the kinetics of the reactions and titrations under study.

The principles elucidated by these studies may be applicable to other classes of reactions as well. For instance, we have previously shown that we can substitute a variety of transition metals^[21] and lanthanides^[22] for the sodium ions in the nanochannels. These materials may serve as catalysts for other types of reactions.

Experimental Section

Instrumentation. ^1H NMR spectra were obtained using a Bruker AMX-300 FT spectrometer (300 MHz) and D_2O as the solvent. Low-angle X-ray diffraction profiles were obtained using an Inel CPS 120 powder diffraction system using monochromated $\text{CuK}\alpha$ radiation. UV/Vis spectra were obtained using a Hewlett-Packard 8453 diode array spectrophotometer. The GC traces were taken with a Hewlett-Packard 5890A gas chromatograph equipped with a Hewlett-Packard Ultra 2 column (length 25 m, diameter 0.2 mm). Measurements of pH were taken using an Accumet Model 15 pH meter.

Materials. Heavily cross-linked LLC matrices of **1** were made as previously described.^[8] The materials were ball-milled to a fine powder, and heated at reflux in distilled THF, captured by filtration, and stored under N_2 . Optima water was obtained from Fisher Scientific, and for air-free operations was degassed by purging with N_2 . THF, ethyl cyanoacetate, and benzaldehyde were purchased from Aldrich Chemical Company, distilled, and stored under N_2 prior to use. All other chemicals were used as purchased.

Catalysis experiments. A sample of the catalyst (ca. 40 mg, 5 mol% based on Na content) was refluxed with benzaldehyde (155 μL , 1.5 mmol) and ethyl cyanoacetate (163 μL , 1.5 mmol) in dry THF (7 mL) with *n*-dodecane (87 μL , 0.38 mmol; internal GC standard). The evolution of products was monitored by GC ($10^\circ\text{C min}^{-1}$, $70 \rightarrow 250^\circ\text{C}$, samples taken after 30, 60, 90, 120, 180, 240, and 420 min). Neat reactions were run at room temperature, quenched after 2 h, and analyzed by GC. Reactions in water were run at reflux for 15–30 min before quenching.

Volumetric titration experiments. A sample of catalyst (ca. 25 mg) was stirred for 48 h with 0.1M acid (1 mL, ca. 2 equiv). Acids used: HCl, cyanoacetic acid, formic acid, acetic acid, pyridinium tosylate, *N*-(2-acetamido)-2-aminoethane-sulfonic acid (ACES), and K_2HPO_4 . For each equilibration with acid, the suspension was centrifuged; and a 0.5-mL aliquot was removed and titrated with standardized 0.01505 M NaOH. The endpoints were detected using a pH meter.

Indicator experiments. An indicator solution was added to a few milligrams of cross-linked LLC and sonicated briefly. For quantitation in water, 10 mg of the heterogeneous base catalyst was stirred with a phenol solution (1 equiv in 2 mL of water) overnight in the absence of air. The resulting

phenoxide concentration was determined from UV/Vis spectroscopy at 288 nm (phenol), 390 nm (3-nitrophenol), 400 nm (4-nitrophenol), or 420 nm (2,4-dinitrophenol), within the linear Beer's Law regime as determined by a four-point calibration curve. For quantitation in THF, the matrix was heated at reflux in the absence of air with 1 equiv of nitrophenol in THF (4 mL) for 2 h. The concentration of phenoxide was measured spectroscopically as above.

Size-exclusion experiments. The cross-linked LLC matrix (10 mg) was stirred with 1 equiv, by cation content, of either Alcian Blue (pyridine variant) or gallamine triethiodide in D₂O (2 mL) in the absence of air. After one day of stirring, the suspensions were centrifuged and an aliquot was analyzed. Alcian Blue (pyridine variant) was analyzed quantitatively by UV/Vis spectroscopy at 615 nm. Measurements were taken within the linear regime for Beer's Law. Gallamine triethiodide concentrations were analyzed by integration of ¹H NMR signals using DMSO as an internal standard.

Received: May 17, 1999 [Z13430IE]

German version: *Angew. Chem.* **1999**, *111*, 3206–3210

Keywords: heterogeneous catalysis • liquid crystals • nanostructures • zeolite analogues

- [1] J. M. Thomas, R. G. Bell, C. R. Catlow, *Handbook of Heterogeneous Catalysis*, Vol. 1 (Eds.: G. Ertl, H. Knozinger, J. Weitkamp), WILEY-VCH, Weinheim, **1997**, pp. 286–387.
- [2] a) G. T. Kokotailo, C. A. Fyfe, *J. Phys. Chem. Solids* **1989**, *50*, 441–447; b) N. Y. Chen, *Catalysis* (Ed.: J. W. Ward) Elsevier, Amsterdam, **1987**, pp. 153–163.
- [3] a) C. T. Kresge, M. E. Leonowicz, W. J. Roth, J. C. Vartuli, J. S. Beck, *Nature* **1992**, *359*, 710–712; b) J. S. Beck, J. C. Vartuli, W. J. Roth, M. E. Leonowicz, C. T. Kresge, *J. Am. Chem. Soc.* **1992**, *114*, 10834–10843.
- [4] a) A. Sayari, *Chem. Mater.* **1996**, *8*, 1840–1852; b) J. Y. Ying, C. P. Mehnert, M. S. Wong, *Angew. Chem.* **1999**, *111*, 58–82; *Angew. Chem. Int. Ed. Engl.* **1999**, *38*, 56–77.
- [5] a) V. A. Russell, C. C. Evans, W. J. Li, M. D. Ward, *Science* **1997**, *276*, 575–579; b) P. Brunet, W. Simard, J. D. Wuest, *J. Am. Chem. Soc.* **1997**, *119*, 2737–2738.
- [6] F. M. Menger, T. Tsuno, *J. Am. Chem. Soc.* **1990**, *112*, 1263–1264.
- [7] J. N. Israelachvili, *Intermolecular and Surface Forces*, Academic Press, London, **1985**.
- [8] D. H. Gray, S. Hu, E. Juang, D. L. Gin, *Adv. Mater.* **1997**, *9*, 731–736.
- [9] The very low water content in the mixture is consistent with an inverse mesophase, and addition of water leads to the expected lamellar structure. See also reference [8].
- [10] J. M. Seddon, *Biochim. Biophys. Acta* **1990**, *1031*, 1–69. Based on the known water content, approximate densities of the materials, and the interchannel distances (from X-ray diffraction), the pore diameters for IH1 and IH2 were calculated to be about 10–15 Å and the wall thicknesses about 30 Å.
- [11] G. Jones, *Org. React.* **1967**, *15*, 204–599.
- [12] a) S. Patai, Y. Israeli, *J. Chem. Soc.* **1960**, 2020–2024; b) S. Patai, Y. Israeli, *J. Chem. Soc.* **1960**, 2024–2030; c) S. Patai, J. Zabicky, *J. Chem. Soc.* **1960**, 2030–2038; d) S. Patai, J. Zabicky, Y. Israeli, *J. Chem. Soc.* **1960**, 2038–2044.
- [13] A. Corma, V. Fornés, R. M. Martín-Aranda, H. García, J. Primo, *Appl. Catal.* **1990**, *59*, 237–248.
- [14] K. R. Kloetstra, H. van Bekkum, *J. Chem. Soc. Chem. Commun.* **1995**, 1005–1006.
- [15] D. J. McQuarrie, D. B. Jackson, *Chem. Commun.* **1997**, 1781–1782.
- [16] a) M. S. Fernandez, P. Fromherz, *J. Phys. Chem.* **1977**, *81*, 1755–1761; b) F. Greiser, C. J. Drummond, *J. Phys. Chem.* **1988**, *92*, 5580–5593; c) O. A. El Seoud, *Adv. Colloid Interface Sci.* **1989**, *30*, 1–30.
- [17] a) S. R. Holmers-Farley, R. H. Reamey, T. J. McCarthy, J. Deutch, G. M. Whitesides, *Langmuir* **1985**, *1*, 725–740; b) S. R. Holmes-Farley, C. D. Bain, G. M. Whitesides, *Langmuir* **1988**, *4*, 921–927; c) J. Wang, L. M. Frostman, M. D. Ward, *J. Phys. Chem.* **1992**, *96*, 5224–5228.
- [18] J. E. Frommer, R. G. Bergman, *J. Am. Chem. Soc.* **1980**, *102*, 5227–534.

- [19] V. Ramesh, H.-S. Chien, M. M. Labes, *J. Phys. Chem.* **1987**, *91*, 5937–5940.
- [20] F. G. Bordwell, *Acc. Chem. Res.* **1988**, *21*, 456–463.
- [21] D. H. Gray, D. L. Gin, *Chem. Mater.* **1998**, *10*, 1827–1832.
- [22] H. Deng, D. L. Gin, R. C. Smith, *J. Am. Chem. Soc.* **1998**, *120*, 3522–3523.
- [23] A. C. O. Hann, A. Lapworth, *J. Chem. Soc.* **1904**, 85, 46–56.

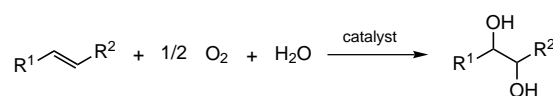
Atom-Efficient Oxidation of Alkenes with Molecular Oxygen: Synthesis of Diols**

Christian Döbler, Gerald Mehlretter, and Matthias Beller*

Dedicated to Professor Manfred Baerns on the occasion of his 65th birthday

The selective oxidation of alkenes with molecular oxygen involving the participation of both oxygen atoms is one of the most significant challenges in modern catalysis research. In spite of the advantages of oxygen over “classical” stoichiometric oxidizing agents (e.g. peracids, chlorates, periodates), only one oxygen atom is generally incorporated into the molecule in the oxidation of alkenes with molecular oxygen. The second oxygen atom reacts with a reducing agent present to form by-products, which are thus formed in stoichiometric amounts. Such processes are found in enzymatic oxidations,^[1] transition metal catalyzed reactions with O₂/H₂, and stoichiometric reactions with O₂/RCHO or O₂/alkylarenes.^[2] Groves et al. have been able for the first time to show that both oxygen atoms of molecular oxygen are used during epoxidation in the presence of a porphyrin–ruthenium catalyst.^[3]

Because of the industrial importance of diols, both as bulk chemicals (in particular propylene glycol)^[4] and as fine chemicals, we are interested in carrying out dihydroxylations with molecular oxygen as oxidant (Scheme 1).



Scheme 1. Metal-catalyzed dihydroxylation with molecular oxygen.

Osmium(VIII) compounds have proved to be the most reliable metal catalysts for dihydroxylations. On the basis of the pioneering work of Sharpless et al.^[5] it has been possible to demonstrate the preparative potential of the method,

[*] Prof. Dr. M. Beller, Dr. C. Döbler, Dipl.-Chem. G. Mehlretter
Institut für Organische Katalysforschung (IfOK)
Buchbinderstrasse 5–6, D-18055 Rostock (Germany)
Fax: (+49) 381-46693-24
E-mail: matthias.beller@ifok.uni-rostock.de

[**] This work was supported by the Bildungsministerium des Landes Mecklenburg-Vorpommern and Bayer AG (Leverkusen). We thank I. Stahr for experimental support, and K. Kortus and Dr. C. Fischer for the GC and HPLC investigations.